Molecular Biology of the Cell
Vol. 15, 121–131, January 2004

The *Drosophila* Kinesin-like Protein KLP67A Is Essential for Mitotic and Male Meiotic Spindle Assembly[V]

Rita Gandhi,* Silvia Bonaccorsi,‡ Diana Wentworth,* Stephen Doxsey,§ Maurizio Gatti,† and Andrea Pereira‡

*Department of Molecular Genetics and Microbiology, §Program in Molecular Medicine, University of Massachusetts Medical School, Worcester, Massachusetts 01655; and ‡Istituto Pasteur-Fondazione Cenci Bolognetti and Istituto di Biologia e Patologia Molecolari del Consiglio Nazionale delle Ricerche , Dipartimento di Genetica e Biologia Molecolare, Universita di Roma "La Sapienza", P.le Aldo Moro 5, 00185 Rome, Italy

Submitted May 29, 2003; Revised August 20, 2003; Accepted August 28, 2003
Monitoring Editor: Ted Salmon

We have performed a mutational analysis together with RNA interference to determine the role of the kinesin-like protein KLP67A in *Drosophila* cell division. During both mitosis and male meiosis, *Klp67A* mutations cause an increase in MT length and disrupt discrete aspects of spindle assembly, as well as cytokinesis. Mutant cells exhibit greatly enlarged metaphase spindle as a result of excessive MT polymerization. The analysis of both living and fixed cells also shows perturbations in centrosome separation, chromosome segregation, and central spindle assembly. These data demonstrate that the MT plus end-directed motor KLP67A is essential for spindle assembly during mitosis and male meiosis and suggest that the regulation of MT plus-end polymerization is a key determinant of spindle architecture throughout cell division.

INTRODUCTION

The proper assembly and positioning of the spindle during both meiosis and mitosis is essential for chromosome segregation and the correct placement of the division plane. Each step of spindle assembly seems to be facilitated by a stochastic state of microtubule (MT) polymerization and depolymerization with intermittent states of pause, termed " dynamic instability" (Mitchison *et al*., 1986). Cytologically, this is manifested as a rapid shrinking and growing of the MT plus ends (the MT minus ends are associated with the centrosomes and are intrinsically more stable). Measurements of MT dynamics in cultured cells (Salmon *et al*., 1984; Saxton *et al*., 1984), as well as in vitro studies with *Xenopus* egg extract (Verde *et al*., 1992), have shown that dynamic instability increases dramatically during entry into mitosis. The dynamic instability of MT plus ends has also been observed in real time during mitosis in yeast (Korinek *et al*., 2000; Lee *et al*., 2000). Together, these observations have led to a model in which dynamic instability allows the MT plus ends to "search and capture" appropriate anchorage sites such as the kinetochores or specialized sites at the cell cortex (Kirschner and Mitchison, 1986; Holy and Leibler, 1994; Desai and Mitchison, 1997; Schuyler and Pellman, 2001).

Article published online ahead of print. Mol. Biol. Cell 10.1091/mbc.E03–05–0342. Article and publication date are available at www.molbiolcell.org/cgi/doi/10.1091/mbc.E03–05–0342.

[V] Online version of this article contains video material for some figures. Online version is available at www.molbiolcell.org.

‡ Corresponding author. E-mail address: andrea.pereira@umassmed.edu.

Many proteins have been discovered that regulate MT dynamic instability (Cassimeris, 1999). The biological role of several kinesin-like proteins in MT dynamics was first made evident by a series of elegant genetic analyses in *S. cerevisiae*. Mutants deficient for the kinesin-like protein *KIP3* were found to be viable but exhibit elongated spindles, and in the absence of dynein, resulted in failures in spindle alignment and nuclear migration (Cottingham and Hoyt, 1997; Straight *et al*., 1998; Cottingham *et al*., 1999). The two fission yeast Kip3p orthologs Klp5p and Klp6p also promote MT destabilization and mutations in these genes affect mitotic chromosome segregation and disrupt meiotic division (West *et al*., 2001, 2002). In vertebrates, the best characterized MT destabilizers are two kinesins of the Kin I family, the *Xenopus* kinesin catastrophe modulator (XKCM1), and its mammalian ortholog mitotic centromere-associated kinesin (MCAK). Inactivation of XKCM1 in *Xenopus* egg extracts results in the formation of large astral arrays of nondynamic, long MTs that are unable to form a bipolar spindle (Walczak *et al*., 1996), whereas overexpression in mammalian cells of specific XKCM1 domains causes MT shortening and perturbs both spindle morphology and chromosome alignment (Kline-Smith and Walczak, 2002; Walczak *et al*., 2002). MCAK, however, may only function at anaphase, because both dominant–negative mutations as well as antisense depletion in cultured cells interfere with chromosome segregation (Maney *et al*., 1998). Although these studies clearly demonstrated that both XKCM1 and MCAK are MT-destabilizing enzymes required for spindle formation and chromosome segregation, they did not determine whether proper MT dynamics is continuously required throughout cell division in higher eukaryotes. This was mainly due to the intrinsic limitations of the systems analyzed (e.g., the

presence of the spindle checkpoint) and to the unavailability of leaky mutations that would allow mutant cells to progress through mitotic division.

Here, we show that the *Drosophila* kinesin-like protein KLP67A is a microtubule-destabilizing factor and that it is continuously required throughout both mitosis and male meiosis. Previous studies have shown that KLP67A is a plus end-directed motor associated with the ends of astral MTs, which is expressed only in proliferative tissues (Pereira *et al*., 1997). Consistent with these results, we show that mutations in *Klp67A* have striking effects on cell division. Our data indicate that proper regulation of MT plus-end polymerization is continuously required throughout cell division, allowing MTs to search and capture their appropriate targets during multiple steps of both mitosis and male meiosis.

MATERIALS AND METHODS

Isolation of Mutations in the Klp67A Gene

To isolate mutations in the *Klp67A* gene, we initially performed a vectorette screen (Eggert *et al*., 1998), starting with *l(3)03691* (Deak *et al*., 1997). We determined by plasmid rescue experiments that *l(3)03691* contains a *P* element at 10 kb from the 3′ end of the *Klp67A* gene. We recovered several new *P* insertions; all located in a "hot spot" 130 base pairs upstream of the transcription start of *Klp67A*. On completion of this screen, a *P* element insertion, *EP(3)3516*, was identified in this same location from the Rorth collection (Rorth, 1996) during the *Drosophila* genome-sequencing project (Spradling *et al*., 1995). Both our insertions and *EP(3)3516* were found to be homozygous viable. They also had no phenotype when made heterozygous with *Df(3L)29A6* that removes *Klp67A*.

To obtain additional *P* element insertions into the KLP67A gene, animals of the genotype *w*; *EP(3)3516/TM6B* were crossed to a strain containing the *P [Δ2-3]* source of *P* transposase. Resulting male progeny of the genotype *w*; *EP(3)3516/P* [Δ*2-3*] were then crossed as single pair matings to *w; Df(3L)29A6/TM6B* females. To screen for local hops, DNA was prepared from pools of *w*; *EP(3)3516/TM6B* progeny, and 200 mutagenized lines were screened by polymerase chain reaction (PCR) with primers specific for *P* and an internal region of *Klp67A*. A size change in the PCR product or its absence indicated a putative deletion. From 200 lines screened, we isolated 20 potential mutations. DNA sequence analysis of several of these lines revealed that they retained the *P* element but contained small deletions of ≤35 base pairs within the promoter region of *Klp67A*. One of these lines, designated $Klp67A^{322b24}$, was then chosen for further characterization. We have determined by reverse transcription (RT)-PCR analysis that in $Klp67A^{322b24}$ mutants transcription begins within the *P* element inserted upstream to the *Klp67A* coding sequence (our unpublished data). However, this change in the site of transcription initiation results only in a slight reduction of the KLP67A level in embryos from mutant mothers (see RESULTS, Figure 4)

Rescue Experiments

A *Klp67A* cDNA was cloned into the *Bam*HI/*Eco*RI sites of the *P* element transformation vector $Pwum^2$ (Heck *et al*., 1993) that allowed KLP67A to be expressed as a fusion protein with a myc epitope at the amino terminus. Germ line transformants with chromosome 2 insertions of $Pwum^2$ [*myc:Klp67A*] were recovered and kept as homozygotes. For rescue crosses, animals of the genotype *w;*$Pwum^2$ [*myc:Klp67A*]; *Df(3L)29A6/TM6B* were crossed to $Klp67A^{322b24}$*/TM6B*; the resulting male progeny *w; Pwum*^{2} *[myc:Klp67A];* $Klp67A^{322b24}$*/Df(3L)29A6* were tested for fertility and found to be completely fertile. The $Pwum^2$ *[myc:Klp67A]* construct was also used to test rescue of extant lethal complementation groups in this region (Leicht and Bonner, 1988). None of these mutations were found to be allelic to *Klp67A*.

Immunofluorescence Analysis of Mutant Testes

Testes were dissected and fixed according to Cenci *et al.* (1994) for α-tubulin and either centrosomin or myosin II immunostaining, and according to Gunsalus *et al.* (1995) for α-tubulin immunostaining followed by actin staining with phalloidin. Fixed preparations were rinsed several times in phosphate-buffered saline (PBS) and then incubated overnight at 4°C with one of the following rabbit primary antibodies, both diluted 1:300 in PBS: anti-centrosomin (Li and Kaufman, 1996), and anti-myosin II (kindly provided by Chris Field, Harvard University, Cambridge, MA). Primary antibodies were detected by 2-h incubation at room temperature with Cy-3 conjugated anti-rabbit Ig-G (SeraLab, Crawley, United Kingdom) diluted 1:30 in PBS. Slides were then incubated for 1 h at room temperature with a monoclonal anti-α-tubulin antibody (Amersham Biosciences, Piscataway, NJ) diluted 1:50 in PBS and then with fluorescein isothiocyanate-conjugated sheep-anti-mouse antisera diluted 1:20 (1 h at room temperature; Jackson ImmunoResearch Laboratories, West Grove, PA). For actin plus tubulin staining, testes were first immunostained for α-tubulin and then incubated with rhodamine-phalloidin (Molecular Probes, Eugene, OR) according to Gunsalus *et al.* (1995). All preparations were mounted with Vectashield H-1200 (Vector Laboratories, Burlingame, CA) and examined with a Zeiss AxioPlan microscope equipped with a 50-W mercury lamp for epifluorescence and with a cooled charge-coupled device (Photometrics, Tucson, AZ). Grayscale digital images were collected using IP Lab Spectrum software and then converted to Photoshop 5.0 format, pseudocolored, and merged.

Live Confocal Imaging

For time-lapse confocal microscopy, early embryos (0–2 h) were manually dechorionated, transferred to adhesive-coated coverslips, and briefly dehydrated to accommodate the addition of injected material. The dehydrated embryos were then covered with halocarbon oil and transferred to the stage of the confocal microscope. A fluorescent conjugate of tubulin (tetramethylrhodamine; Cytoskeleton, Denver, CO) was then microinjected into the embryos at a concentration of 5 μg/ml. The behavior of the labeled tubulin was visualized directly using a Leica TCS-SP laser-scanning confocal microscope as described previously (Theurkauf and Heck, 1999).

RNA Interference

Drosophila cultured cells (DL2) were grown at room temperature in Schneider's *Drosophila* medium supplemented with 10% fetal bovine serum and 1× penicillin streptomycin solution. For transfection, cells were cultured at 2×10^5 cells/ml in a 24-well dish with and without coverslips for ~18 h before transfection. Cells were transfected by standard calcium phosphate method with 5 μg *Klp67A* dsRNA per well in 1 ml of medium. After 16–18 h of transfection, cells were washed with fresh medium and cultured for another 24 h before fixation or RT-PCR. Cells were fixed in methanol and immunostained with fluorescein isothiocyanate conjugated anti-α-tubulin (1:200 dilution; Sigma-Aldrich, St. Louis, MO), 4,6-diamidino-2-phenylindole (DAPI) (Sigma-Aldrich), and an antibody to ATP synthase (1:2000 dilution; gift of R. Garesse, Universidad Autonoma de Madrid, Spain).

For Western blot analysis, equivalent concentrations of total cell proteins were separated on SDS gels and transferred to polyvinylidene difluoride (Bio-Rad, Hercules, CA). Protein concentrations were determined using a bicinchoninic acid protein assay kit (Pierce Chemical, Rockford, IL). Blots were probed with a rabbit anti-KLP67A antiserum directed against the peptide YEDFDQDTESDSEELHRTFKR. To standardize protein concentrations of different samples, blots were also probed with the anti-α-tubulin monoclonal antibody E7 at a 1:10 dilution (DSHB, Department of Biology, University of Iowa, Iowa City, IA). Horseradish peroxidase-conjugated secondary antibodies (Jackson ImmunoResearch Laboratories) were used at a 1:5000 dilution, and binding was detected by chemiluminescence (PerkinElmer Life Sciences, Boston, MA).

For synthesizing double-stranded RNA (dsRNA), a 500-base pair fragment of *Klp67A* was PCR amplified using gene-specific primers (5′-T7-AGTACG-GCCGTATAATGTCCGTG-3′ and 5′-T7-CCACTGACCACCACGCCATTG-3′). These primers each contained a contiguous 5′ T7 Promoter sequence (5′-TTAATACGACTCACTATAGGGAGA-3′) to allow in vitro transcription from both strands of the 500-base pair *Klp67A* PCR fragment. For synthesizing *Klp61F* dsRNA, gene-specific primer (5′-T7-GACGGGCACAGGGAAGAC-CCAC-3′ and 5′T7-TCCCTTTTCATTCCCAGCCTTGG-3′) were used. An Ambion MEGAscript TM T7 kit (catalog no. 1334) was used for the in vitro transcription reaction. The RNA was precipitated with lithium chloride and dissolved in water. It was annealed by heating at 94°C for 1 min and allowed to cool down gradually for 18 h. The quality of dsRNA was checked on a 1% agarose gel and quantified by UV spectrophotometry. For RT-PCR, the RNA was isolated from cells by using QIAGEN RNeasy mini kit and amplified using QIAGEN one-step RT-PCR kit with *Klp67A* gene-specific primers (5′-CGAAAACCAAACAAGAGC-3′ and 5′-CCCACATCGAATTTGCGC-3′) and *Klp61F*-specific gene primers (5′-TGGGTACCGACATATCTGGTGG-GAATACG-3′ and 5-GTGGGTCTTCTCTGTGCCCGTC-3′).

RESULTS

The Meiotic Phenotype of Klp67A Mutants

To determine the phenotypic consequences of reducing the level of KLP67A during meiotic division, we used males bearing the $Klp67A^{322b24}$ mutation over *Df(3L)29A6*, which removes $Klp67A^{+}$. In these hemizygous males, the KLP67A level is reduced compared with homozygous $Klp67A^{322b24}$ males, leading to almost complete sterility. *Df(3L)29A6/+* males are completely fertile and do not exhibit any meiotic defect (see below), indicating that heterozygosity for *Df(3L)29A6* does not contribute to the mutant phenotype. To determine the cellular basis of the sterility phenotype, testes

from *Klp67A*^{322b24}/*Df(3L)29A6* males were dissected, squashed, and examined cytologically for the presence of meiotic defects. As shown in Figures 1-3, a number of MT-related defects occur throughout all stages of the first meiotic division. First, in 89% (n = 74) of late prophase figures (stage M1 according to Cenci *et al*., 1994), the asters are not properly positioned at the opposite sides of the nucleus as in wild type (Figure 1A) but ectopically localized in the cytoplasm and close to each other (Figure 1B); occasionally, centrosomes and their associated asters seem to detach from the poles, giving rise to asters that freely float in the cytoplasm (Figure 1C). Despite this defect in aster localization and separation, most *Klp67A* primary spermatocytes (96%; n = 52) progressively assemble a bipolar spindle, which has the ability to mediate the formation of a metaphase plate (Figure 2C, arrowhead) and to proceed through anaphase (Figure 2C, arrow). However, mutant metaphase and anaphase spindles both display astral MTs that seem to be longer than their wild-type counterparts. In addition, in 12% of anaphase figures (n = 25), the two daughter nuclei have different sizes, suggesting an aberrant chromosome segregation (Figure 2C, arrow). Telophase I spindles of *Klp67A* spermatocytes are even more irregular. In 60% (n = 60) of these telophase figures, astral MTs are longer than in wild-type and the central spindle is either absent or much less dense than that seen in normal cells (Figure 2, D and E). An examination of secondary spermatocytes undergoing the second meiotic division revealed that only 18% of late prophase figures (n = 60) exhibit ectopic aster localization. However, cells in subsequent stages of meiosis II show the same defects observed in primary spermatocytes undergoing meiosis I (our unpublished data). Interestingly, 47% of ana-telophase II figures (n = 132) display two spindles within the same cytoplasm (Figure 2G), suggesting a failure of cytokinesis during the first meiotic division. In these "double" secondary spermatocytes astral MTs are also long, so that MTs from asters of different spindles often overlap, resulting in a highly disorganized spindle architecture (Figure 2G).

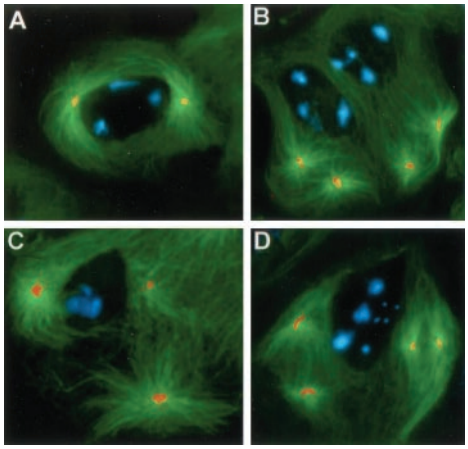

Figure 1. Klp67A is required for aster migration to the opposite sides of spermatocyte nuclei. Wild-type (A) and *Klp67A*^{322b24}/*Df(3L)29A6* (B–D) Primary spermatocyte preparations were stained for α-tubulin (green), centrosomin (red), and DNA (blue). (A) Prometaphase I spermatocyte showing two well separated prominent asters closely apposed to the nuclear envelope. (B) Two mutant prometaphase I spermatocytes with ectopically located asters, not associated with the nuclear envelope and still close to each other. (C) A mutant primary spermatocyte showing the bulk of one of the centrosomes and its associated aster detached from the spindle pole (arrowhead). (D) Tetraploid mutant spermatocyte with four ectopically located asters, indicating a cytokinesis failure in a previous gonial division.

To characterize the cytokinetic phenotype of *Klp67A* mutants, spermatocytes were stained for myosin II and F actin, two well-known components of the contractile ring. As can be seen in Figure 3, A and C, wild-type spermatocytes exhibit a robust central spindle and a clear acto-myosin ring. Mutant telophases with a normal central spindle also exhibit a regular contractile ring (our unpublished data). In contrast, mutant telophases with a poorly organized central spindle display a diffuse actin and myosin staining at the cleavage furrow rather than the typical tight band seen in wild-type cells (Figure 3, B and D). These results indicate that *Klp67A* telophases with a defective central spindle are unable to assemble a contractile ring and to undergo cytokinesis.

To determine the outcome of the spindle defects observed in *Klp67A* mutant spermatocytes, we analyzed spermatid morphology. In wild type, both chromosomes and mitochondria are equally partitioned between the two daughter cells at each meiotic division. After completion of meiosis, the mitochondria fuse to form a conglomerate called the nebenkern. Thus, each wild-type spermatid consists of a round phase-light nucleus associated with a single phase-dark nebenkern of similar size (Figure 3E). Defects in chromosome segregation result in differently sized nuclei (Gonzalez *et al*., 1989), whereas failures in cytokinesis give rise to spermatids that comprise a large nebenkern associated with either two or four normal-sized nuclei (Fuller, 1993). An examination of *Klp67A* mutant spermatids revealed that 41% of these cells (n = 254) have large nebenkern associated with two or four nuclei (Figure 3, F and G). In addition, we found that 24% of the nuclei display irregular sizes (Figure 3G). Together, these observations strongly suggest that *Klp67A* spermatocytes are defective in both chromosome segregation and cytokinesis.

Finally, it should be noted that we observed a few polyploid spermatocytes with four rather than two centrosomes (Figure 1D). This finding suggests that KLP67A is also required for cytokinesis during the gonial mitoses that precede meiotic division. Both the sterility and the meiotic phenotypes are completely rescued by a *Pwum*^{2} [*myc*:*Klp67A*] transgene (see MATERIALS AND METHODS).

Klp67A Maternal Effect on Embryonic Divisions

Females of the genotypes *Klp67A*^{322b24}/*Df(3L)29A6* exhibit reduced fertility compared with the parent strains *Klp67A*^{322b24}/*TM6B* and *Df(3L)29A6/TM6B*. Forty percent of the eggs laid by *Klp67A*^{322b24}/*Df(3L)29A6* females hatch to first instars compared with 96% of the eggs laid by a wild-type strain. However, eggs laid by *Klp67A*^{322b24}/*Df(3L)29A6* females exhibit only a small decrease in the amount of the KLP67A protein compared with those from either the parent strains or wild type, indicating that the *Klp67A*^{322b24} mutation reduces gene expression only slightly (Figure 4A). Nonetheless, the reduction in KLP67A caused by this mutation is sufficient to lower female fertility and to cause mitotic defects in embryonic divisions (see below).

To determine whether the partial sterility of *Klp67A*^{322b24}/*Df(3L)29A6* females is due to a defect in the early blastoderm mitoses, eggs from *Klp67A*^{322b24}/*Df(3L)29A6* mothers crossed to wild-type males were collected and used for real-time analysis of mitosis in living embryos. Rhodamine-labeled tubulin was injected into living embryos and mitosis was allowed to proceed in real time. Time-lapse analysis showed that both spindle formation and architecture is severely abnormal through all stages of mitosis (Figures 4 and

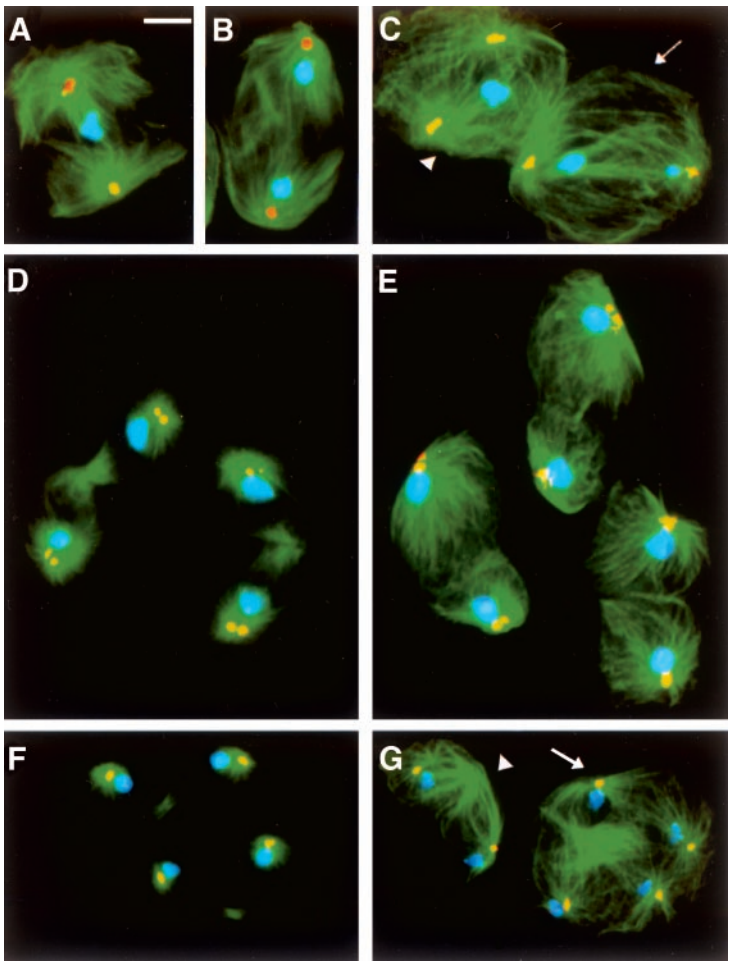

Figure 2. Klp67A mutations affect spindle morphology of *Drosophila* spermatocytes. Wild-type (A, B, D, and F) and *Klp67A*^{322b24}/*Df(3L)29A6* (C, E, and G) meiotic cells were stained for α-tubulin (green), centrosomin (orange), and DNA (blue). (A) Wild-type metaphase I. (B) Wild-type anaphase I. (C) A mutant metaphase (arrowhead) with a bipolar spindle and an anaphase figure (arrow) showing an abnormal chromosome segregation. In both cells, the MTs seem to be longer than in their wild-type counterparts. (D) Two wild-type telophases I. (E) Three mutant telophases I showing abnormally long astral MTs and defective central spindles. (F) Two wild-type telophases II. (G) Mutant telophases II. The arrowhead points to a morphologically abnormal telophase figure in which interpolar MTs overlap in the middle of the cell but do not form a typical dense central spindle. The arrow points to two telophases within the same cytoplasm showing long astral MTs. Note the overlapping of astral MTs emanating from different spindles. Bar, 10 μm.

5; see also Video 1 in Supplemental Material). Control embryos derived from *Df(3L)29A6/TM6B* mothers undergo normal mitoses, as shown in Video 2 (Supplemental Material).

The first important feature of the mutant phenotype is seen during prophase, when the majority of the centrosomes do not complete their migration to the opposite sides of the nucleus (Figure 4A, arrows). The average angle between prophase centrosomes (n = 60) was observed to be 145.2° in mutants and 164.2° in controls (n = 54). Although this difference is small, it is statistically significant according to the Student's t test (p = 0.0002). Incompletely separated centrosomes then give rise to curved banana-shaped metaphase spindles (Figure 4B). The centrosome migration defect is sometimes seen even in wild-type embryonic cells, where it results in the same misshapen spindle phenotype observed in mutant embryos (Figure 4; Videos 1 and 2 in Supplemental Material). However, in mutant embryos this spindle malformation not only occurs more frequently but it is also exacerbated. Videos 1 and 2 in Supplemental Material, from which Figures 4 and 5 are derived, also reveal that the distortion of the normal shape of the spindle occurs when dynamic MTs seem to reach the chromosomes. At this precise moment, the spindle becomes distorted and banana shaped to accommodate the extended MTs emanating from the spindle poles (see below). In addition, in some mutant prometaphase and metaphase spindles (video 1) centrosomes detach from the spindle poles, as occurs during male meiosis. The timing of centrosome separation is also affected by a reduction in KLP67A. The period of centrosome migration up until the point of nuclear envelope breakdown lasts for at least 3 min; 1 min longer than in wild-type embryos.

A second important feature of mutant metaphase spindles is their increased length compared with wild-type spindles. The average pole-to-pole distance in mutant metaphases (n = 60) is 15.6 μm ($\pm$1.5 SD), compared with 10.3 μm ($\pm$0.64 SD) in wild-type metaphases (n = 54). It is important to note that this increased spindle length is observed in all mutant spindles and is not a consequence of the defect in centrosome separation, because even the spindles with normal centrosome positioning are longer than their wild-type counterparts (Figure 5, 290 s; Videos 1 and 2 in Supplemental Material). In addition, in all types of spindles, the increase in pole-to-pole distance is associated with an increase in MT length. Thus, these results suggest that the activity of KLP67A is required for limiting the length of spindle MTs.

A third important feature of the *Klp67A* maternal effect phenotype is seen during telophase, when most spindles seem to be either missing a normal central spindle or have a greatly reduced number of midzone MTs (Figure 5, 370 s). Central spindle formation normally occurs during anaphase when the overlapping set of antiparallel interpolar MTs become bundled (Mastronarde *et al*., 1993). Although areas of MT overlap can be seen in the central region of most of these mutant spindles (Figure 5), their midzone MTs are not organized in the typical dense lateral array that characterizes wild-type central spindles. This suggests that the abnormally long, and often curved or bent, astral MTs are not able to interact properly to give rise to the ordered parallel array

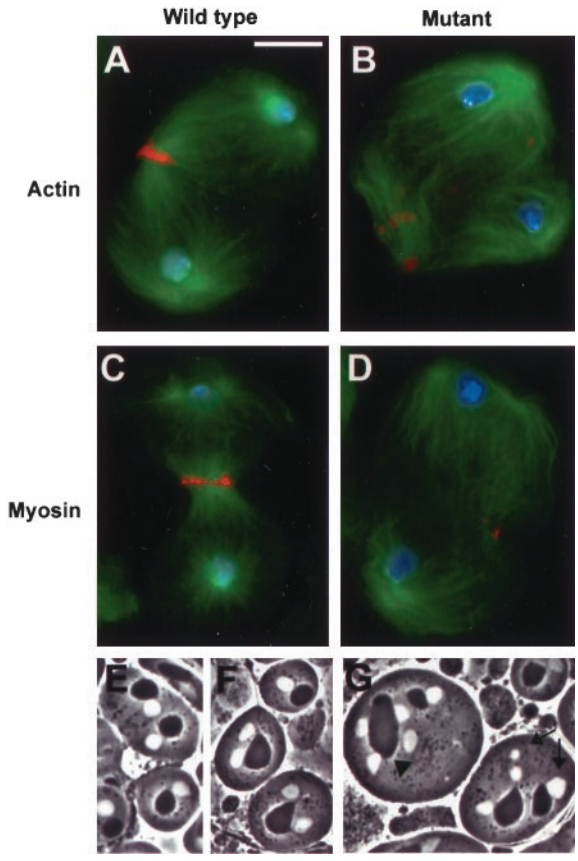

Figure 3. Klp67A mutations disrupt central spindle and contractile ring assembly and cause failures in both cytokinesis and chromosome segregation. Primary spermatocytes from wild-type (A and C) and *Klp67A*^{322b24}/*Df(3L)29A6* (B and D) males. Preparations were stained for α-tubulin (green), actin (A and B; red) or myosin (C and D; red) and DNA (blue). (A and C) Wild-type telophase I spermatocytes showing a prominent central spindle and a regular actomyosin ring. (B and D) Mutant telophase I figures showing a severely defective central spindle and irregular patches of either actin (b) or myosin (d) at the cleavage furrow. (E–G) Phase contrast images of wild-type (e) and *Klp67A*^{322b24}/*Df(3L)29A6* (F and G) living spermatids. (E) Wild-type partial cyst in which each spermatid consists of a phase-dark nebenkern and a phase-light nucleus. (F) *Klp67A* mutant spermatids consisting of two equally sized nuclei associated with a large nebenkern (G) A *Klp67A* spermatid consisting of a large nebenkern associated with four nuclei of normal size (arrowhead) and two spermatids showing irregularly sized nebenkern associated with micro- and macronuclei (arrows). Bar, 10 μm.

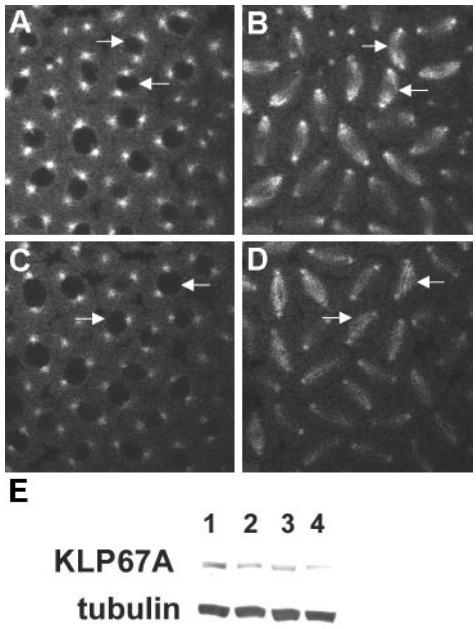

Figure 4. Klp67A mutations cause an incomplete centrosome separation. (A–D) Still images from real-time analysis of mitosis in blastoderm embryos of *Klp67A*^{322b24}/*Df(3L)29A6* (A and B) and wild-type (C and D) mothers. Note the correlation between incomplete centrosome separation and curved banana-shaped spindles (arrows). Incomplete centrosome separation is sometimes seen in wild-type (arrows in C), which also results in curved spindle (arrows in D) but is less frequent than in the mutant. (E) Western blot analysis of KLP67A expression. Protein homogenates were prepared from 0 to 2.5 h egg collections from mutant and wild-type mothers. The blot was probed with a rabbit polyclonal antibody to KLP67A as well as an antibody to α-tubulin. α-Tubulin was used as a loading control. 1, wild-type control. 2, *Df(3L)29A6/TM6B.* 3, *Klp67A*^{322b24}*/TM6B.* 4, *Klp67A*^{322b24}*/Df(3L)29A6*.

of central spindle MTs. Because these early blastoderm mitoses do not require MTs to form the pseudocleavage furrow (Stevenson *et al*., 2001), aberrant spindles are often able to proceed through telophase and two daughter spindles can form in the ensuing divisions. Chromosome behavior has also been observed in eggs laid by *Klp67A*^{322b24}/*Df(3L)29A6* females by using real-time analysis of eggs injected with Oligreen. Surprisingly, in spite of the structural abnormalities observed in the spindles of these eggs, chromosome segregation seems normal (Video 4, Supplemental Material).

To analyze spindle dynamics in *Klp67A* mutant embryos, Videos 1 and 2 in Supplemental Material were used to calculate the interval between nuclear envelope breakdown (t = 0 s) and the appearance of a central spindle (albeit drastically abnormal in the mutant embryo). As shown in Figure 5B, this period lasts 2 min longer in mutant embryos (360 s) than in wild-type embryos (240 s). This difference is primarily due to an increase in the amount of time spent in metaphase and anaphase B. Figure 5B also shows that, during metaphase, the mutant spindles continue to increase in length, whereas their wild-type counterparts reach a plateau. In addition, the final spike in pole separation at anaphase B occurs later (at 300 s) than in wild-type (at 220 s). Although wild-type and mutant spindles do not exhibit a noticeable difference in the speed of chromosome movement during anaphase A (Videos 3 and 4 in Supplemental Material), the mutant spindles take significantly longer to go through anaphase B (90 s in mutants versus 30 s in wild type). This slowing of anaphase B may be related to the unusual S-shaped conformation assumed by mutant spindles during pole separation (Figure 5A, 370 s).

Western blot analysis of eggs derived from *Klp67A*^{322b24}/*Df(3L)29A6* mothers demonstrated that the *Klp67A*^{322b24} allele lowers gene expression only slightly (Figure 4E). This suggests that MT polymerization and, as a result, spindle assembly is extremely sensitive to a slight decrease in the level of KLP67A during both male meiosis and embryonic mitosis.

RNAi of Klp67A

A genetic null allele of *Klp67A* would greatly facilitate the functional analysis of this gene. Because at this time, a null allele is unavailable, RNAi was used to create a severely

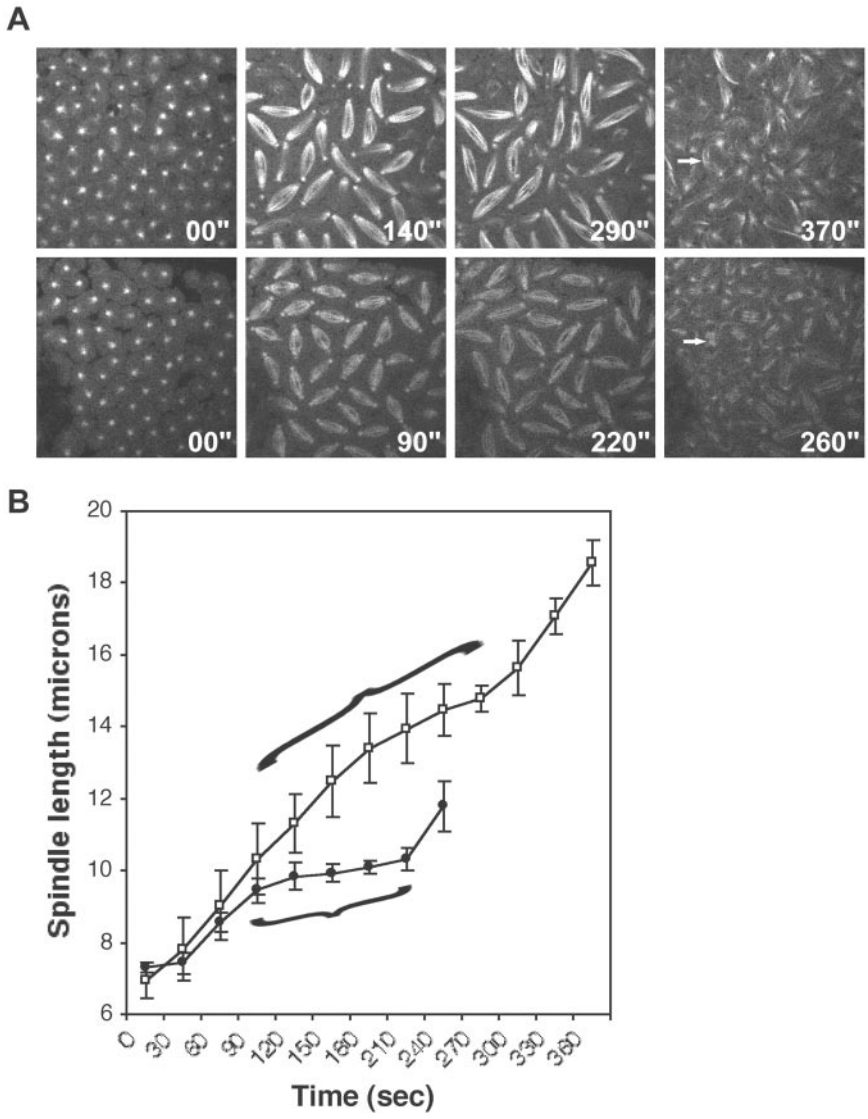

Figure 5. Klp67A mutations result in abnormally long and curved spindles and a failure of central spindle assembly. (A) Mutant embryos (*Klp67A*^{322b24}/*Df(3L)29A6*; top four panels) and wild-type embryos [*Df(3L)29A6/TM6B*; bottom four panels] were injected with rhodamine-tubulin, and mitotic divisions were examined by time-lapse confocal microscopy. Panels show representative images of different mitotic stages; timing is indicated at the bottom of each panel. Note that the mutant spindles are abnormally long and curved and that midzone MTs are not apparent during anaphase B in the mutant as they are in wild type (arrows). (B) Plot of spindle length versus time beginning with nuclear envelope breakdown up until central spindle formation at the end of anaphase B of cycle 11. Note that mutant spindles are consistently longer that their wild-type counterparts and that there is a significant lengthening of the time spent in metaphase (compare bracketed intervals). Bar, SD; closed circles, wild-type; empty squares, mutant.

hypomorphic *Klp67A* mutant. These experiments were performed using the DL2 cell line of *Drosophila*. The flat morphology of these cells allows a clear view of individual MTs, permitting a reliable evaluation of the effect of KLP67A on MT length. For these experiments, cells were transfected with a 500-base pair double-stranded *Klp67A* RNA and examined 42–44 h after the beginning of dsRNA treatment (see MATERIALS AND METHODS). Depletion of *Klp67A* mRNA as well as the KLP67A protein was demonstrated by RT-PCR and Western blot analysis (Figure 6, E and F). Transfected and mock-transfected cells were fixed, stained for both tubulin and DNA, and analyzed for defects in mitotic division (Figure 6). The frequency of cells in the different stages of mitosis in treated versus control cells is shown in Table 1. It is evident from these data that RNAi causes a mitotic block at metaphase. This suggests that cells treated with *Klp67A* dsRNA are unable to progress to anaphase and telophase, probably due to the activation of the mitotic checkpoint that prevents cells with defective spindles to enter anaphase (see DISCUSSION).

Although the metaphase arrest of *Klp67A* dsRNA-treated cells precludes observation of the entire mitotic process, certain aspects of the phenotype of these cells resemble the *Klp67A* maternal effect observed in blastoderm embryos. The spindles of dsRNA-transfected cells are extremely elongated as in the blastoderm embryo. Several examples of these spindle malformations can be seen in Figure 6. The pole-to-pole distance in the control spindle shown in Figure 6A is less than half of that observed in the RNAi spindles shown in Figure 6, B–D (note that all these images are at the same magnification). These enlarged spindles also show interpolar MTs that seem abnormally long and curved. In addition, the overall shape of these spindles is often curved as in the blastoderm mitotic divisions, again indicating incomplete centrosome separation. The metaphase chromosome configuration is also abnormal and a tight metaphase plate arrangement is rarely seen. All of these phenotypes are consistent with an increased MT length and stability caused by the ablation of the *Klp67A* gene activity. Furthermore, concentrations of nocadazole that destabilize MTs and perturb spindle assembly in control DL2 cells only slightly affect spindle architecture and have no effect on astral MT arrays in KLP67A-depleted cells (Gandhi and Pereira, unpublished data). The RNAi phenotype observed in cultured cells is likely to correspond to that elicited by a strong mutant allele. RT-PCR analysis has shown that the *Klp67A* dsRNA treat-

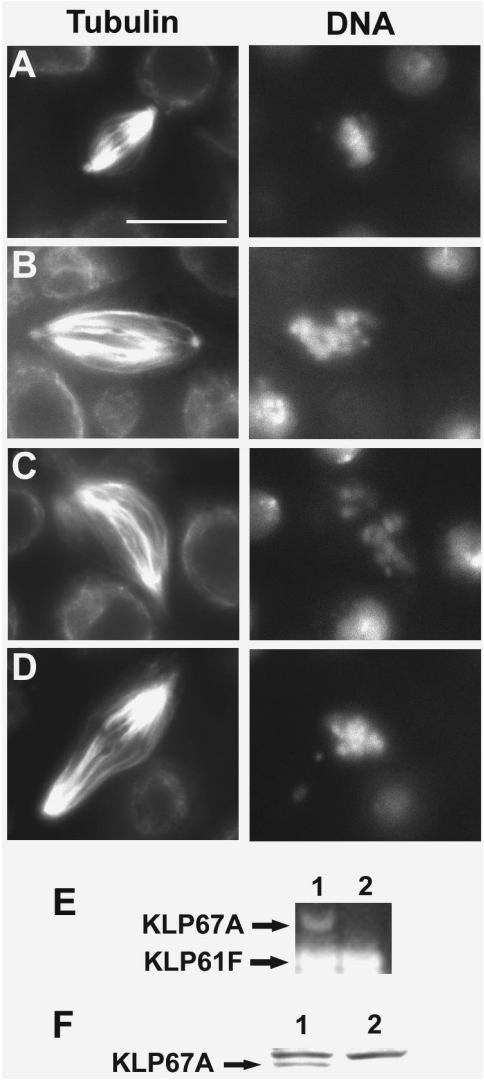

Figure 6. Klp67A dsRNA treatment in DL2 cells results in elongated spindles and mitotic arrest. (A–D) Cytological phenotypes caused by KLP67A depletion. *Klp67A* (RNAi) cells and control cells were fixed and stained for α-tubulin and DNA (with DAPI). (A) Mock-transfected control cells. (B–D) Cells treated with *Klp67A* dsRNA. (A) Metaphase. (B–D) Metaphase-like spindles in RNAi cells. Bar, 10 μm. (E) Semiquantitative RT-PCR assay shows undetectable levels of *Klp67A* mRNA in dsRNA-treated samples. 1, control; 2, cells treated with *Klp67A* dsRNA. *Klp61F* mRNA amplified by RT-PCR was used as an internal control. (F) Western blot analysis of DL2 cells treated with *Klp67A* dsRNA. Forty micrograms of protein was loaded in each lane, and the blot was probed with a rabbit polyclonal antibody to KLP67A. The common background band serves as a loading control.

ment results in a significant decrease in the *Klp67A* mRNA after two days of treatment (Figure 6E).

Because previous studies showed that KLP67A is associated with mitochondria at the plus ends of astral microtubules (Pereira *et al*., 1997), we also examined whether KLP67A depletion affects mitochondria distribution in DL2 cells. An antibody to ATP synthase was used to visualize mitochondria in control and dsRNA-treated cells. In control cells, mitochondria surround metaphase spindles displaying a rather uniform distribution, consistent with their association with the ends of the astral MTs (Figure 7A). However,

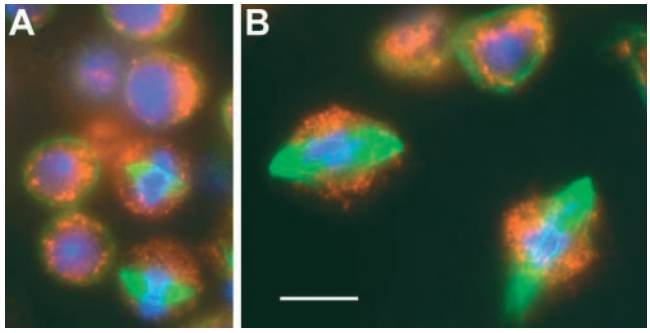

Figure 7. KLP67A depletion affects the mitochondria distribution pattern in DL2 cells. *Klp67A* (RNAi) cells were fixed and stained with anti-α-tubulin (green), anti-F1ATP synthase (red) to stain mitochondria, and DAPI (blue). (A) Mock-transfected control cells. (B) Cells treated with *Klp67A* dsRNA. Bar, 10 μm.

in KLP67A-depleted cells mitochondria seem to be excluded from the cell poles and concentrated around the metaphase plate (Figure 7B). It is important to note that these cells are forced to assume an elongated shape to accommodate the enlarged mutant spindles, whereas control metaphase cells exhibit a typical round shape (Figure 7). As a consequence of this deformation, the astral MTs of KLP67A-depleted cells are not found in their normal radial array but are forced inward, so that their plus ends are all oriented toward the chromosomes (Figure 7B). The characteristic distribution of mitochondria in KLP67A-depleted cells is therefore likely to be a secondary consequence of the altered cell shape. In mutant precellular blastoderm embryos, where the astral arrays are not constricted by a cell membrane, this abnormal mitochondria distribution is not seen (Pereira, unpublished data).

Double RNAi of Klp67A and Klp61F

The increase in MT length observed in *Klp67A* mutant cells could indicate a requirement for KLP67A in the regulation of MT growth. Alternatively, KLP67A could be required for maintaining normal spindle pole separation, and the increased pole-to-pole distance in *Klp67A* mutant cells could result in an increased MT polymerization. To discriminate between these possibilities, we examined whether the absence of KLP67A results in abnormal MT elongation in monopolar spindles. To perform this analysis, DL2 cells were cotransfected with both *Klp61F* dsRNA and *Klp67A* dsRNA. Previous genetic analyses (Heck *et al*., 1993) and antibody injection experiments (Sharp *et al*., 1999a) have shown that KLP61F depletion prevents centrosome separation, resulting in monopolar spindles. As predicted, treatment of DL2 cells with *Klp61F* dsRNA does indeed produce frequent spindles with unseparated asters. These monopolar spindles are associated with highly condensed chromosomes that seem to be in metaphase (Figure 8). Double RNAi treatment with *Klp61F* and *Klp67A* effectively reduced the expression of both mRNAs (Gandhi and Wentworth, unpublished data) and also resulted in monopolar spindles. However, these monopolar spindles display a dramatic increase in MT length compared with those observed in cells transfected with *Klp61F* dsRNA alone (Figure 8). In addition, in cells doubly depleted for KLP61F and KLP67A, the individual MT fibers of monopolar spindles are not only much longer than those in KLP61F-depleted monopolar spindles, but they are also often curved (Figure 8) as those observed in mutant *Klp67A* embryos. It is also noteworthy that the effect

Table 1. RNAi of *Klp67A* results in metaphase arrest

	Mitotic index	No. of mitotic figures	Prophase %	Prometaphase %	Metaphase %	Anaphase %	Telophase %
Control	3.4[a]	85	17.6	12.9	52.9	8.2	8.2
Klp67A (RNAI)	13.1[b]	252	3.6	23.8	69.8	1.5	1.1

DL2 cells were transfected with *Klp67A* dsRNA or mock transfected (control). The mitotic index is percentage of cells in mitosis, recorded after 2 d since the beginning of dsRNA treatment.

[a] n = 2430.

[b] n = 1923.

of KLP67A on MT length is observed as early as in prometaphase and in some cases even in prophase (Figure 8, arrow). The finding that the activity of KLP67A is required as early as prophase indicates that the increased MT length seen in mutant spindles is not an indirect consequence of the metaphase arrest phenotype.

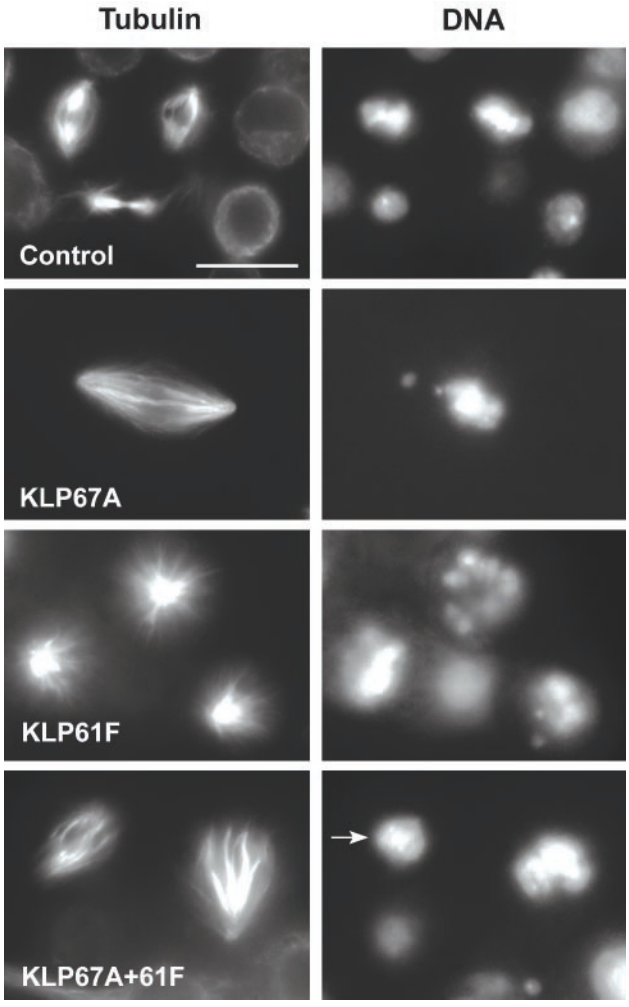

Figure 8. Depletion of both KLP61F and KLP67A arrests cells in mitosis with monopolar spindles. DL2 cells were transfected with *Klp67A* dsRNA and *Klp61F* dsRNA, either separately or in combination. Cells were fixed and stained for α-tubulin and DNA (with DAPI). Note the monopolar spindle morphology in cells treated with either *Klp61F* dsRNA alone or with both *Klp67A* and *Klp61F* dsRNA. In the latter case, MTs are much longer than in the former. Bar, 10 μm.

DISCUSSION

Our functional analyses have demonstrated a requirement for KLP67A in the regulation of MT growth and stability during both *Drosophila* mitosis and male meiosis. Depletion of this MT plus end-directed motor increases the length and perturbs the morphology of spindle MTs, beginning as early as prophase and extending through ana-telophase. Normally, mitotic MTs are known to be much shorter and less stable than interphase MTs (Salmon *et al*., 1984; Saxton *et al*., 1984). Studies with *Xenopus* egg extracts have indicated that the mechanism for this change in MT stability is an increase in the frequency of transitions from MT polymerization to depolymerization at the MT plus ends (reviewed in Desai and Mitchison, 1997). Thus, KLP67A may affect MT stability during both mitosis and male meiosis through either a direct or indirect effect on MT dynamics.

It has been proposed that the Kip3 family, which includes KLP67A, shares a close evolutionary relationship with the Kin I family and that they may be functional orthologs (Severin *et al*., 2001). However, other sequence homology studies strongly suggest a significant divergence (Endow and Kim, 2000; Miki *et al*., 2001). Based on sequence similarity, the Kip3 family can be subdivided into the fungal and metazoan subfamilies (West *et al*., 2001). The fungal subfamily of Kip3 is comprised of the *Saccharomyces cerevisiae* Kip3p and *Schizosaccharomyces pombe* Klp5p and Klp6p. The fungal members are further characterized by conserved domains at their amino terminal ends and in their tail domains that are not shared with their metazoan Kip3 relatives (West *et al*., 2001). The metazoan subfamily includes the *Drosophila* KLP67A, mouse KIF18A and KIF18B, LF22F4 of *C. elegans* as well as other representatives (Endow and Kim, 2000; Miki *et al*., 2001). Further evidence suggesting the functional divergence of the Kip3 family from the Kin I family comes from biochemical studies. Unlike the Kin I family kinesins, KLP67A does not depolymerize taxol-stabilized MTs nor does it have an internal catalytic domain (Pereira *et al*., 1997). In addition, whereas Kin I family kinesins, such as MCAK, diffuse along the MTs (Hunter *et al*., 2003), KLP67A is a directional motor that moves toward the MT plus ends (Pereira *et al*., 1997).

Although, the KLP67A and the fungal Kip3 members have a similar in vivo effect on MT stability and length (Cottingham and Hoyt, 1997; DeZwaan *et al*., 1997; Cottingham *et al*., 1999; West *et al*., 2001), the fact that they are in different subfamilies is likely to pertain to the specific requirements

for MT stability in spindle assembly and function in metazoans. Unlike the yeast cellular phenotype, the *Drosophila* phenotype includes a dramatic and global increase in spindle size, problems in aster separation and chromosome segregation and defects in central spindle formation. Furthermore, whereas *KIP3* is inessential for yeast mitosis, the function of KLP67A is essential for somatic cell division, as a "knock-down" of *Klp67A* results in a nearly complete mitotic arrest. KLP67A is also required for male meiosis like the *S. pombe* Kip3 family members, but unlike the *S. cerevisiae* Kip3p.

We have analyzed the phenotypic consequences of KLP67A depletion in three different *Drosophila* cell types: blastoderm embryonic cells, spermatocytes, and DL2 cultured cells. Because the depletion of KLP67A in cultured cells results in an almost complete mitotic arrest, null mutations of *Klp67A* are predicted to be lethal. In contrast, flies bearing the $Klp67A^{322b24}$ hypomorphic allele over a deficiency that removes $Klp67A^{+}$ are viable, albeit partially sterile. Therefore, this allelic combination results in a level of KLP67A that is sufficient to sustain development to adulthood but is just at the threshold for normal MT dynamics and spindle assembly in spermatocytes and early embryos. At this time, the biochemical mechanism, which explains how a small decrease in the level of KLP67A in the embryo can lead to such a dramatic effect in MT behavior, is unknown. However, because male meiosis and precellular blastoderm mitosis are highly suitable systems for observing cell division in *Drosophila*, the availability of the hypomorphic $Klp67A^{322b24}$ allele has been extremely advantageous to the functional analysis of KLP67A.

The absence of a stringent spindle checkpoint in embryonic cells and spermatocytes was also advantageous to our phenotypic analysis. We have shown that mutant embryonic cells and spermatocytes both proceed through anaphase and telophase, in contrast to KLP67A-depleted DL2 cells that arrest at metaphase. We believe that these findings reflect the different stringencies of the spindle checkpoint mechanisms that are operating in these three cell types. During male meiosis, the spindle checkpoint is known to be weak and only causes a small delay in the anaphase onset in response to the presence of univalent chromosomes (Rebollo and Gonzalez, 2000) and does not prevent spermatocytes with severely malformed spindles to undergo anaphase and telophase (Bonaccorsi *et al*., 1998; Sampaio *et al*., 2001; Wakefield *et al*., 2001; Riparbelli *et al*., 2002). Similarly, in the early blastoderm embryo, a stringent checkpoint is not operating until the midblastula (Sibon *et al*., 1997). In contrast, it is likely that DL2 cells employ a stringent checkpoint that prevents cells with defective spindles to enter anaphase. A similar checkpoint has been observed in larval neuroblasts that arrest in metaphase in response to the spindle defects caused by mutations in the *abnormal spindle* gene (Basto *et al*., 2000). Except for this checkpoint-mediated arrest, the three types of cells examined respond in similar ways to the depletion of KLP67A. All cell types display a substantial increase in MT length and an abnormal centrosome separation. In addition, blastoderm embryos and spermatocytes, the two systems with nonstringent checkpoints, fail to organize a normal central spindle. However, whereas blastoderm embryos exhibit normal chromosome segregation, a substantial fraction of both primary and secondary spermatocytes are defective in this process. We suggest that all these phenotypic abnormalities depend on the same primary defect in the regulation of MT plus-end polymerization.

Our data demonstrate that there is a defect in centrosome separation during both mitosis and male meiosis in *Klp67A* mutant cells. Two other *Drosophila* MT motors have previously been shown to participate in centrosome separation. Mutations in the cytoplasmic dynein heavy chain gene *Dhc64D* result in a maternal effect phenotype that includes incomplete centrosome separation and frequent centrosome loss (Robinson *et al*., 1999). Because Dhc64D is cortically located, it has been suggested to power centrosome separation during prophase by exerting a minus-end directed "reeling in" force on astral MTs (Sharp *et al*., 1999a). Another *Drosophila* motor required for centrosome separation is the bimC family member, KLP61F (Heck *et al*., 1993; Sharp *et al*., 1999a,b). Antibody injection experiments in *Drosophila* embryos have led to the suggestion that this bipolar kinesin is not needed for powering aster migration but for maintaining aster separation (Sharp *et al*., 1999c). Our data suggest that the centrosome separation defect in KLP67A-depleted cells results from changes in MT dynamics and disproportionate MT growth. It is likely that in these cells the improper behavior of the plus ends of astral MTs prevents the MT–cortex interactions that mediate centrosome migration to the opposite poles of the nucleus. Thus, even though Dhc64D and KLP67A play distinct roles in centrosome separation, defects in either function would reduce astral pulling forces resulting in incomplete centrosome separation.

Chromosome segregation in the *Klp67A* mutant blastoderm seems normal, but this process is affected in both meiotic divisions of *Klp67A* mutant males. The finding that spermatocytes require KLP67A for chromosome segregation is not surprising, as the abnormal MT behavior observed in the mutants can account for problems in chromosome segregation. However, we do not understand why blastoderm cells, despite the defect in MT dynamics, normally segregate their chromosomes. The simplest explanation for this discrepancy is that spermatocytes and blastoderm cells have different requirements for normal chromosome segregation. These cell-specific requirements may be related to the duration of cell division in these two types of cells. In the extremely rapid mitotic process of blastoderm cells chromosome segregation could indeed be mediated by molecular mechanisms that are partially different from those used during meiotic divisions.

We have found that *Klp67A* mutations disrupt central spindle formation in both blastoderm embryos and spermatocytes. Central spindle formation is known to be mediated by plus end-directed MT cross-linking kinesins, such as Pavarotti (Adams *et al*., 1998), the *Drosophila* homolog of MKLP1. It is thus likely that the cross-linking activities of these kinesins require the function of KLP67A to ensure correct MT plus-end dynamics and morphology during central spindle assembly. However, although we favor the view that KLP67A only acts as a MT-depolymerizing factor, our results do not exclude the possibility that KLP67A has an additional MT bundling activity, promoting central spindle assembly in concert with the other MT cross-linking kinesins. In blastoderm embryos the defect in central spindle does not result in a failure to separate the two daughter nuclei, because the formation of the pseudocleavage furrow is a MT-independent process (Stevenson *et al*., 2001). However, in spermatocytes the defect in central spindle is accompanied by a failure to assemble a normal contractile apparatus and to undergo cytokinesis. This is consistent with a large body of data indicating that in animal cells, including *Drosophila*, proper central spindle assembly is an essential prerequisite for contractile ring formation (Gatti *et al*., 2000).

Previous observations on *Drosophila* embryos showed that KLP67A is associated with a population of tiny mitochondria at the plus ends of astral microtubules (Pereira *et al*., 1997). We found that in KLP67A-depleted cells mitochondria concentrate at the plus ends of MTs (Figure 7), consistent with previous studies, indicating that mitochondria use multiple motors to attach themselves to MTs (Nangaku *et al*., 1994; Tanaka *et al*., 1998). However, mitochondria seem to have different distributions in control and in KLP67A-depleted metaphase cells (Figure 7). In the latter cells, they are more highly concentrated in the center of the spindle than in control cells. This is most likely a secondary effect of the abnormal aster morphology in KLP67A-depleted metaphases, with the long astral MTs extending inward rather than radially (see RESULTS). However, our results do not exclude the possibility that mitochondria mispositioning may contribute to the increased MT stability observed in mutant cells.

To summarize, our data suggest that the plus end-directed KLP67A motor acts at the MT plus ends where it either directly or indirectly promotes MT destabilization. We propose that KLP67A activity is required for spindle MTs to interact properly during centrosome migration, metaphase spindle formation, chromosome segregation, and central spindle assembly when MT ends must dynamically search and capture their appropriate targets. Further studies are underway to define the precise effect of KLP67A on MT dynamics during cell division.

ACKNOWLEDGMENTS

We thank Bill Theurkauf for generously allowing us to use his confocal microscope. We especially thank Byeong Cha for technical assistance during the embryo injections, and Paul Furcinitti (University of Massachusetts Bio Imaging Core Facility) for technical help in imaging. We also thank Tom Kaufman, Chris Field, and R. Garesse for the gifts of the cnn, myosin, and ATP-synthase antisera, respectively. This work was supported by the National Institutes of Health (R01521411) as well as an American Heart Association Award (525314) to A.J.P., and by grants from Fondo per gli investimenti della Ricerca di Base (RBNE01KXC9-004) and Centro di Eccellenza di Biologia e Medicina Molecolare to M.G. A.J.P. and R.G. thank Paul R. Dobner and Amitabh Mohanty for invaluable assistance. A.J.P. also thanks William S. Gelbart (Harvard University) for laboratory space during the initiation of this project.

REFERENCES

Adams, R.R., Tavares, A.A., Salzberg, A., Bellen, H.J., and Glover, D.M. (1998). *pavarotti* encodes a kinesin-like protein required to organize the central spindle and contractile ring for cytokinesis. Genes Dev. *12*, 1483–1494.

Basto, R., Gomes, R., and Karess, R.E. (2000). Rough Deal and Zw10 are required for the metaphase checkpoint in *Drosophila.* Nat. Cell Biol. *2*, 939–943.

Bonaccorsi, S., Giansanti, M.G., and Gatti, M. (1998). Spindle self-organization and cytokinesis during male meiosis in *asterless* mutants of *Drosophila melanogaster.* J. Cell Biol. *142*, 751–761.

Cassimeris, L. (1999). Accessory protein regulation of microtubule dynamics throughout the cell cycle. Curr. Opin. Cell Biol. *11*, 134–141.

Cenci, G., Bonaccorsi, S., Pisano, C., Verni, F., and Gatti, M. (1994). Chromatin and microtubule organization during premeiotic meiotic, and early postmeiotic stages of *Drosophila melanogaster* spermatogenesis. J. Cell Sci. *107*, 3521–3534.

Cottingham, F.R., Gheber, L., Miller, D.L., and Hoyt, M.A. (1999). Novel roles for *Saccharomyces cerevisiae* mitotic spindle motors. J. Cell Biol. *147*, 335–349.

Cottingham, F.R., and Hoyt, M.A. (1997). Mitotic spindle positioning in *Saccharomyces cerevisiae* is accomplished by antagonistically acting microtubule motor proteins. J. Cell Biol. *138*, 1041–1053.

Deak, P., *et al*. (1997). P-element insertion alleles of essential genes on the third chromosome of *Drosophila melanogaster*: correlation of physical and cytogenetic maps in chromosomal region 86E–87F. Genetics *147*, 1697–1722.

Desai, A., and Mitchison, T.J. (1997). Microtubule polymerization dynamics. Annu. Rev. Cell Dev. Biol. *13*, 83–117.

DeZwaan, T.M., Ellingson, E., Pellman, D., and Roof, D.M. (1997). Kinesin related *KIP3* of *Saccharomyces cerevisiae* is required for a distinct step in nuclear migration. J. Cell Biol. *138*, 1023–1040.

Eggert, H., Bergemann, K., and Saumweber, H. (1998). Molecular screening for P-element insertions in a large genomic region of *Drosophila melanogaster* using polymerase chain reaction mediated by the vectorette. Genetics *149*, 1427–1434.

Endow, S. A. and Kim, A. J. (2000). The kinesin tree. http://www.blocks.fhcrc.org/%7Ekinesin/

Fuller, M.T. (1993). Spermatogenesis. In: The Development of *Drosophila* melanogaster, vol. I., ed. M. Bate and A.M. Arias, Plainview, NY: Cold Spring Harbor Laboratory Press, 71–147.

Gatti, M., Giansanti, M.G., and Bonaccorsi, S. (2000). Relationships between the central spindle and the contractile ring during cytokinesis in animal cells. Microsc. Res. Tech. *49*, 202–208.

Gonzalez, C., Casal, J., and Ripoll, P. (1989). Relationship between chromosome content and nuclear diameter in early spermatids of *Drosophila melanogaster*. Genet. Res. *54*, 205–212.

Gunsalus, K., Bonaccorsi, S., Williams, E., Verni, F., Gatti, M., and Goldberg, M. (1995). Mutations in *twinstar*, a *Drosophila* gene encoding a cofilin/ADF homologue, result in defects in centrosome migration and cytokinesis. J. Cell Biol. *131*, 1243–1259.

Heck, M.M.S., Pereira, A., Pesavento, P., Yannoni, Y., Spradling, A.C., and Goldstein, L.S.B. (1993). The kinesin-like protein KLP61F is essential for mitosis in *Drosophila.* J. Cell Biol. *123*, 665–679.

Holy, T.E., and Leibler, S. (1994). Dynamic instability of microtubules as an efficient way to search in space. Proc. Nat. Acad. Sci. USA *91*, 5682–5685.

Hunter, A.W., Caplow, M., Coy, D.L., Hancock, W.O., Diez, S., Wordeman, L., and Howard, J. (2003). The kinesin-related protein MCAK is a microtubule depolymerase that forms an ATP-hydrolyzing complex at microtubule ends. Mol. Cell *11*, 445–457.

Kirschner, M., and Mitchison, T. (1986). Beyond self-assembly: from microtubules to morphogenesis. Cell *45*, 329–342.

Kline-Smith, S.L., and Walczak, C.E. (2002). The microtubule-destabilizing kinesin XKCM1 regulates microtubule dynamic instability in cells. Mol. Biol. Cell *13*, 2718–2731.

Korinek, W.S., Copeland, M.J., Chaudhuri, A., and Chant, J. (2000). Molecular linkage underlying microtubule orientation toward cortical sites in yeast. Science *287*, 2257–2259.

Lee, L., Tirnauer, J.S., Li, J., Schuyler, S.C., Liu, J.Y., and Pellman, D. (2000). Positioning of the microtubule spindle by a cortical-microtubule capture mechanism. Science *287*, 2260–2262.

Leicht, B.L., and Bonner, J.J. (1988). Genetic analysis of chromosomal region 67A-D of *Drosophila melanogaster*. Genetics *119*, 579–593.

Li, K., and Kaufman, T.C. (1996). The homeotic target gene centrosomin encodes an essential centrosomal component. Cell *85*, 585–596.

Maney, T., Hunter, A.W., Wagenbach, M., and Wordeman, L. (1998). Mitotic centromere-associated kinesin is important for anaphase chromosome segregation. J. Cell Biol. *142*, 787–801.

Mastronarde, D.N., McDonald, K.L., Ding, R., and McIntosh, J.R. (1993). Interpolar spindle microtubules in PTK cells. J. Cell Biol. *123*, 1475–1489.

Miki, H., Setou, M., Kaneshiro, K., and Hirokawa, N. (2001). All kinesin superfamily protein, KIF, genes in mouse and human. Proc. Nat. Acad. Sci. USA *98*, 7004–7011.

Mitchison, T.J., Evans, L., Schulze, E., and Kirschner, M. (1986). Sites of microtubule assembly and disassembly in the mitotic spindle. Cell *45*, 515–527.

Nangaku, M., Sato-Yoshitake, R., Okada, Y., Noda, Y., Takemura, R., Yamazaki, H., and Hirokawa, N. (1994). KIF1B, a novel microtubule plus end-directed monomeric motor protein for transport of mitochondria. Cell *79*, 1209–1220.

Pereira, A.J., Dalby, B., Stewart, R.J., Doxsey, S.J., and Goldstein, L.S.B. (1997). Mitochondrial association of a plus end-directed microtubule motor expressed during mitosis in *Drosophila.* J. Cell Biol. *136*, 1081–1090.

Rebollo, E., and Gonzalez, C. (2000). Visualizing the spindle checkpoint in *Drosophila* spermatocytes. EMBO Rep. *1*, 65–70.

Riparbelli, M.G., Callaini, G., Glover, D.M., and Avides Mdo, C. (2002). A requirement for the Abnormal Spindle protein to organize microtubules of the central spindle for cytokinesis in *Drosophila.* J. Cell Sci. *115*, 913–922.

Robinson, J.T., Wojcik, E.J., Sanders, M.A., McGrail, M., and Hays, T.S. (1999). Cytoplasmic dynein is required for nuclear attachment and migration of centrosomes during mitosis in *Drosophila*. J. Cell Biol. *146*, 597–608.

Rorth, P. (1996). A modular misexpression screen in *Drosophila* detecting tissue-specific phenotypes. Genetics *93*, 12418–12422.

Salmon, E.D., Leslie, R.J., Saxton, W.M., Karrow, M.L., and McIntosh, J.R. (1984). Spindle microtubule dynamics in sea urchin embryos: analysis using a fluorescein-labeled tubulin and measurements of fluorescence redistribution after laser photobleaching. J. Cell Biol. *99*, 2165–2174.

Sampaio, P., Rebollo, E., Varmark, H., Sunkel, C.E., and Gonzalez, C. (2001). Organized microtubule arrays in gamma-tubulin-depleted *Drosophila* spermatocytes. Curr. Biol. *11*, 1788–1793.

Saxton, W.M., Stemple, D.L., Leslie, R.J., Salmon, E.D., Zavortink, M., and McIntosh, J.R. (1984). Tubulin dynamics in cultured mammalian cells. J. Cell Biol. *99*, 2175–2186.

Schuyler, S.C., and Pellman, D. (2001). Search, capture and signal: games microtubules and centrosomes play. J. Cell Sci. *114*, 247–255.

Severin, F., Habermann, B., Huffaker, T., and Hyman, T. (2001). Stu2 promotes mitotic spindle elongation in anaphase. J. Cell Biol. *153*, 435–442.

Sharp, D.J., Brown, H.M., Kwon, M., Rogers, G.C., Holland, G., and Scholey, J.M. (1999a). Functional coordination of three mitotic motors in *Drosophila* embryos. Mol. Biol. Cell *11*, 241–253.

Sharp, D.J., McDonald, K.L., Brown, H.M., Matthies, H.J., Walczak, C., Vale, R.D., Mitchison, T.J., and Scholey, J.M. (1999b). The bipolar kinesin, KLP61F, cross-links microtubules within interpolar microtubule bundles of *Drosophila* embryonic mitotic spindles. J. Cell Biol. *144*, 125–138.

Sharp, D.J., Yu, K.R., Sisson, J.C., Sullivan, W., and Scholey, J.M. (1999c). Antagonistic microtubule-sliding motors position mitotic centrosomes in *Drosophila* early embryos. Nat. Cell Biol. *1*, 51–54.

Sibon, O.C., Stevenson, V.A., and Theurkauf, W.E. (1997). DNA-replication checkpoint control at the *Drosophila* midblastula transition. Nature *388*, 93–97.

Spradling, A.C., Stern, D., Kiss, I., Roote, J., Laverty, T., and Rubin, G.M. (1995). Gene disruptions using *P* transposable elements. Proc. Natl. Acad. Sci. USA *92*, 10824–10830.

Stevenson, V.A., Kramer, J., Kuhn, J., and Theurkauf, W.E. (2001). Centrosomes and the Scrambled protein coordinate microtubule-independent actin reorganization. Nat. Cell Biol. *3*, 68–75.

Straight, A.F., Sedat, J.W., and Murray, A.W. (1998). Time-lapse microscopy reveals unique roles for kinesins during anaphase in budding yeast. J. Cell Biol. *143*, 687–694.

Tanaka, Y., Kanai, Y., Okada, Y., Nonaka, S., Takeda, S., Harada, A., and Hirokawa, N. (1998). Targeted disruption of mouse conventional kinesin heavy chain, kif5B, results in abnormal perinuclear clustering of mitochondria. Cell *93*, 1147–1158.

Theurkauf, W.E., and Heck, M.M. (1999). Identification and characterization of mitotic mutations in *Drosophila.* Methods Cell Biol. *61*, 317–346.

Verde, F., Dogterom, M., Stelzer, E., Karsenti, E., and Leibler, S. (1992). Control of microtubule dynamics and length by cyclin-A and cyclin-B dependent kinases in *Xenopus* egg extracts. J. Cell Biol. *118*, 1097–1108.

Wakefield, J.G., Bonaccorsi, S., and Gatti, M. (2001). The *Drosophila* protein Asp is involved in microtubule organization during spindle formation and cytokinesis. J. Cell Biol. *153*, 637–648.

Walczak, C.E., Gan, E.C., Desai, A., Mitchison, T.J., and Kline-Smith, S.L. (2002). The microtubule-destabilizing kinesin XKCM1 is required for chromosome positioning during spindle assembly. Curr. Biol. *12*, 1885–1889.

Walczak, C.E., Mitchison, T.J., and Desai, A. (1996). XKCM *1*, A *Xenopus* kinesin-related protein that regulates microtubule dynamics during mitotic spindle assembly. Cell *84*, 37–47.

West, R.R., Malmstrom, T., and McIntosh, J.R. (2002). Kinesins klp5^{+} and klp6^{+} are required for normal chromosome movement in mitosis. J. Cell Sci. *115*, 931–940.

West, R.R., Malmstrom, T., Troxell, C.L., and McIntosh, J.R. (2001). Two related kinesins, klp5+ and klp6+, foster microtubule disassembly and are required for meiosis in fission yeast. Mol. Biol. Cell *12*, 3919–32.